ELSEVIER

Journal of Power Sources 66 (1997) 129–133

JOURNAL OF POWER SOURCES

Studies on Li–Mn–O spinel system (obtained from melt-impregnation method) as a cathode for 4 V lithium batteries Part IV. High and low temperature performance of $LiMn_2O_4$

Yongyao Xia, Masaki Yoshio *

Department of Applied Chemistry, Saga University, Saga 840, Japan

Received 17 September 1996; accepted 21 October 1996

Abstract

The cycling profile of an Li/1 M $LiPF_6$ + ethylene carbonate/dimethyl carbonate (1:2 in volume)/$LiMn_2O_4$ cell is examined at various operating temperatures (0, 25 and 50 °C). The capacity fades faster on cycling at a high operating temperature than that at a low one. It is found that the two-phase structure in a high-voltage region is very sensitive to the working temperature. This two-phase structure can be stably maintained for lithium-ion insertion/extraction at a low temperature in the high-voltage region, while it is effectively forced to transform to a more stable one-phase structure at high temperatures. The capacity loss at high operating temperature is due to the following factors: (i) an unstable two-phase structure co-exists in the high-voltage region for lithium-ion insertion/extraction; (ii) Mn slowly dissolves in the electrolyte solution, and (iii) the electrolyte solution decomposes on the electrode.

Keywords: Lithium; Lithium-ion batteries; Spinel; Manganese dioxide

1. Introduction

It has been demonstrated that the spinel-structure lithium manganese oxide is the most promising positive-electrode material for lithium-ion batteries because of its economic and environmental advantages. The rechargeability has been greatly improved [1–3]. Although, capacity fading on charge/discharge cycling is also observed, these optimum spinel electrodes can maintain more than 120 mAh g^{-1} over extensive cycling at room temperature. For commercial applications, however, it is typically expected that batteries will have to operate at various temperatures. What will occur if the Li/$LiMn_2O_4$ cell works in a high-temperature environment? What are the problems and how are they solved? Accordingly, this investigation examines the electrochemical behaviour of Li/$LiMn_2O_4$ cells at low and high operating temperatures.

2. Experimental

The compound under examination was prepared by reaction of LiOH and MnO_2 at 470 °C for 5 h under an oxygen flow, followed by heating at 750 °C for 20 h in air by the melt-impregnation method [3].

The chemical composition was determined by chemical analysis [4]. The crystal structure was determined using a Rigaku RINT1000 X-ray diffractometer (Rigaku, Japan) with Fe Kα radiation, monochromated by a graphite crystal.

Charge/discharge tests and cycle-life tests were examined in CR2030 button-type cells. The cell consisted of a positive electrode and a lithium-metal negative electrode separated by a porous polypropylene film. Metallic lithium was in excess. The mixture, which contained 25 mg active material and 15 mg conducting binder (Teflonized acetylene black), was pressed on a 2.0 cm^2 stainless-steel screen. The electrolyte used was 1 M $LiPF_6$–ethylene carbonate (EC)/dimethyl carbonate (DMC) (1:2 in volume).

The a.c. impedance measurements were performed with a Solartron Instrument Model 1287 electrochemical interface and a 1250 B frequency response analyser controlled by a COMPAQ PC computer. The frequency limits were typically set between 60 KHz to 0.01 Hz. The a.c. oscillation was 10 mV.

3. Results and discussion

3.1. Characterization of $LiMn_2O_4$

The chemical composition of the resulting compound was determined to be $LiMn_2O_4$ (Li%, Mn%, MnO_2%, y in MnO_y

* Corresponding author.

PII S0378-7753(96)02538-4

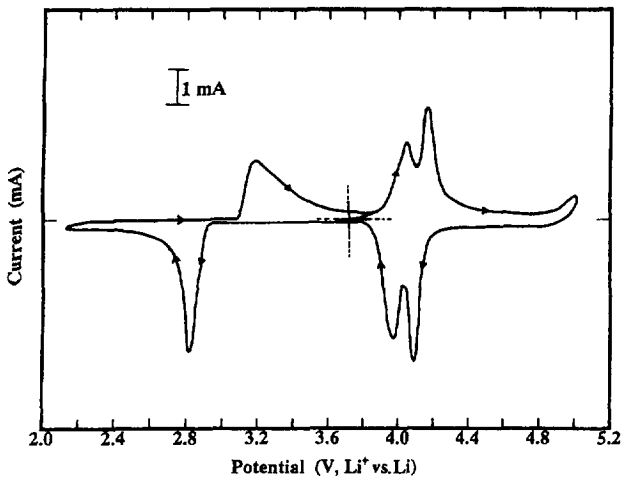

Fig. 1. Cyclic voltammogram for $LiMn_2O_4$ at 25 °C. Potential scanned at a rate of 10 mV min^{-1} between 2.0 and 5.0 V.

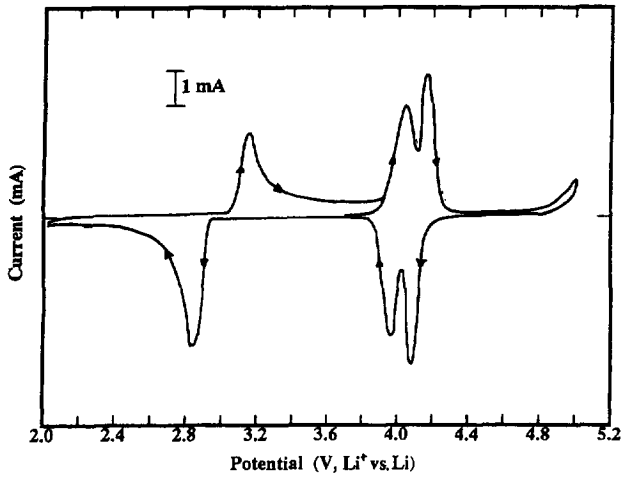

Fig. 2. Cyclic voltammogram for $LiMn_2O_4$ at 50 °C. Potential scanned at a rate of 10 mV min^{-1} between 2.0 and 5.0 V.

are 3.84, 60.77, 72.12 and 1.751%, respectively) by chemical analysis and atomic adsorption spectroscopy. The crystal structure was indexed to a cubic system with a lattice parameter a_0 of 8.24 Å, which is refined with space group *Fd3m*. The structure can be described as layers of close-packed oxygen, in which lithium and manganese ions occupy 8*a* tetrahedral sites and 16*d* octahedral sites, respectively. A cyclic voltammogram for this electrode cycled between 2.0 and 5.0 V is shown in Fig. 1. One pair of peaks in the 3 V region and two pairs of peaks in the 4 V region, corresponding to lithium-ion extraction/insertion in octahedral sites and tetrahedral sites, are observed. These results agree well with the results reported by Rossouw et al. [5]. Here, it should be pointed out that neither an additional peak at around 3.9 V versus Li/Li^+ (discharge), which is due to the appearance of a new structure or to electronic modification [6], nor a peak located at 4.5 V caused by Mn presence in 8*a* tetrahedral sites [1] were observed on this sample. The cyclic voltammogram for this electrode at 50 °C is given in Fig. 2. There are no major differences from the voltammogram obtained at 25 °C (Fig. 1), even in the high-voltage region. It seems that the electrolyte solution is stable up to 4.8 V (Li^+ versus Li) against oxidation for an electrode of such composition. Thus, it is possible to exclude the possibility that electrolyte decomposition causes the capacity loss on cycling when the cell is cycled between 3.5 and 4.5 V at room or high operating temperatures. It should be pointed, however, that cyclic voltammetry is unable to detect the decomposition of small amounts of electrolyte. Hence, it is still necessary to determine whether the solution decomposes, or not. This can be decided by using the a.c. impedance technique, which is very sensitive to the interface reaction (see Section 3.5).

3.2. Charge and discharge profile

A typical charge/discharge curve for the Li/$LiMn_2O_x$ cell at a current rate of *C*/3 at 25 °C is given in Fig. 3. The electrode has an initial charge capacity of 140 mAh g^{-1},

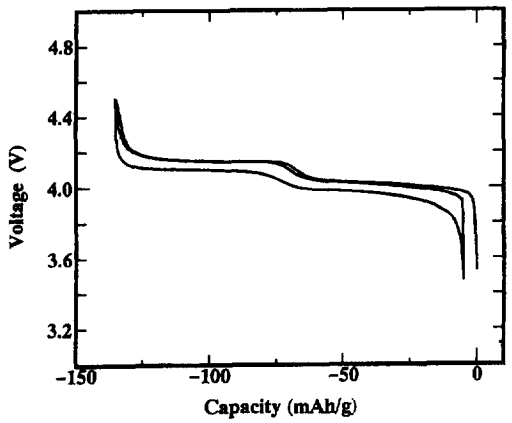

Fig. 3. Typical charge and discharge curves for Li/$LiMn_2O_4$ cell at a current of *C*/3 at 25 °C.

which is close to the theoretical value (148 mAh g^{-1}). This shows that about 0.94 mole Li^+ was extracted from the spinel matrix, corresponding to a composition of $Li_{0.06}Mn_2O_4$. The electrode also delivers a reversible capacity of 134 mAh g^{-1} with a two-step voltage profile. The cell containing the spinel cathode has a low electrode polarization, namely, < 50 mV.

3.3. Cycling performance at various operating temperatures

The relationship between specific capacity and cycle number of a Li/$LiMn_2O_4$ coin cell cycled at a current rate of *C*/3 between 3.5 and 4.5 V at various operating temperatures is plotted in Fig. 4. The capacity fading on cycling is faster at an operating temperature of 50 °C, which loses about 19% of the initial discharge capacity of 130 mAh g^{-1}, compared with 8 and 4% for the cell at 25 and 0 °C for the first 50 cycles, respectively.

3.4. Capacity fading on cycling

The charge curves for Li/$LiMn_2O_4$ at 50 and 0 °C are shown in Fig. 5(a) and (b), respectively. Two phenomena are clearly observed for the cell operated at 50 °C:

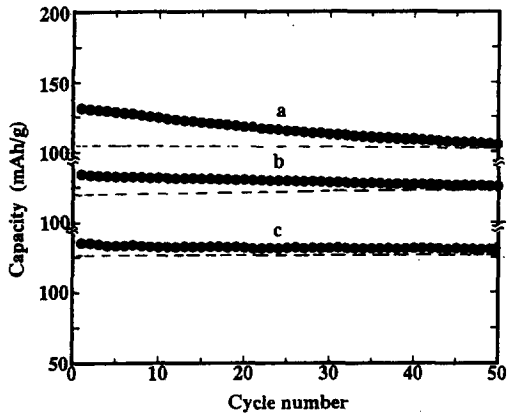

Fig. 4. Cycling behaviour of Li/1 M $LiPF_6$–EC/DMC (1:2 in volume)/ $LiMn_2O_4$ at various operating temperatures: (a) 50 °C; (b) 25 °C, and (c) 0 °C.

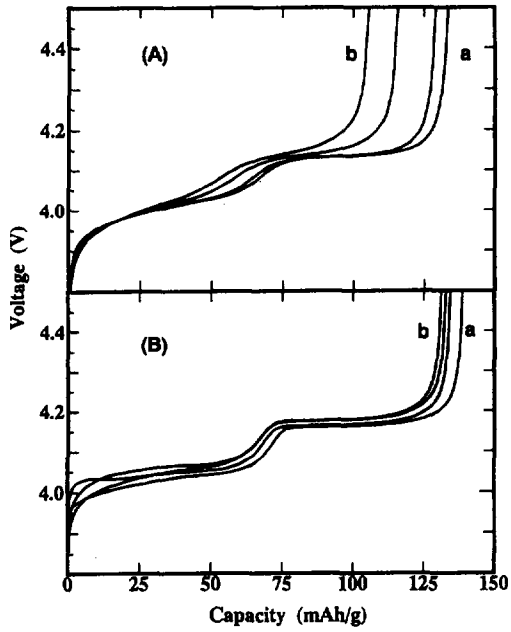

Fig. 5. Charge curves (1st, 5th, 25th and 50th) between 3.8 and 4.5 V for Li/$LiMn_2O_4$ at: (A) 50 °C; (B) 0 °C. (a) 1st, and (b) 50th charge.

(i) the capacity loss occurs mainly in the high-voltage region (over 4.1 V in charge); here is little capacity loss in the low-voltage region, which is different behaviour to that of the cell cycled at room temperature [7] where the capacity loss occurs only in the high-voltage region;

(ii) the shape of the charge curve in the high-voltage region is gradually changed to an 'S shape' from an 'L shape' for the cell at 50 °C.

The phenomena can be seen more clearly in Fig. 6 that reports the results for Li/$LiMn_2O_4$ coin cells cycled between 3.5 and 4.12 V at 25 and 50 °C. The charge voltage was limited to 4.12 V. This means that the cell was only cycled in the low-voltage region in which only a one-phase structure exists [7]. As expected, the cell cycled at 25 °C does not lose capacity (curve (a) in Fig. 6); this is in agreement with previous work [7]. The results indicate that the crystal structure of $LiMn_2O_4$ in the low-voltage region is stable for Li^+

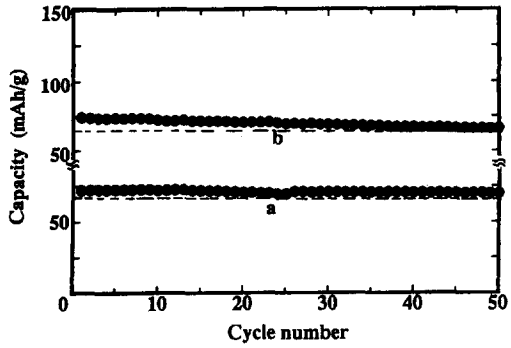

Fig. 6. Cycling behaviour of Li/1 M $LiPF_6$ – EC/DMC (1:2 in volume)/ $LiMn_2O_4$ at various operating temperatures between 3.5 and 4.12 V: (a) 25 °C, and (b) 50 °C.

insertion/extraction, while the rechargeable capacity of the cell cycled at 50 °C reduces from 74 to 66 mAh g^{-1} in the low-voltage region. What, therefore, causes the capacity loss for the cell cycled between 3.5 and 4.5 V at 50 °C? One possibility is a slow dissolution of Mn into the electrolyte solution. Preliminary chemical analysis results show that about 5% $LiMn_2O_4$ dissolves into the electrolyte solution after 50 cycles at 50 °C. This suggests that the capacity loss caused by Mn dissolution accounts for only 25% of the overall capacity loss. In fact, the mechanism of Mn dissolution has not yet been clarified. It is still not known whether the Mn dissolution is caused simply by the disproportionation reaction $2Mn^{3+} \rightarrow Mn^{4+} + Mn^{2+}$ or not [8] since the capacity occurs dominantly in the high-voltage region, where the Mn^{3+} content in spinel oxides is minimal. Further investigations are required.

The remaining portion (75%) of the capacity loss could be caused by other unfavourable effects. One is due to an unstable two-phase structure co-existing in the high-voltage region for lithium-ion insertion/extraction [6], because the L-shaped curve gradually transforms to an S-shaped curve. Another effect could be electrolyte solution decomposition, which will be confirmed by a.c. impedance experiments in following section. At this stage, it is difficult to determine which process dominates the capacity loss. By comparing the changes in curve shape between the cell cycled at 50 and 0 °C (Fig. 5(b)), it is found that the charge curve after cycling at 0 °C still retains an L shape. This suggests that the two-phase structure in the high-voltage region can stably co-exist at low temperature, but a high temperature effectively forces a transformation to a one-phase structure in the high-voltage region. Hence, it is concluded that the capacity loss for the cell cycled at 50 °C is mainly due to an unstable two-phase structure, because changes in structure depend on the cycled temperature, and it is easily envisaged that the capacity loss due to an unstable two-phase structure co-existing in the high-voltage region is more serious at the high operating temperature than that at the low operating temperature. Based on this, one route to improve the high-temperature performance of a spinel electrode material is to replace $LiMn_2O_4$ with non-stoichiometric spinel, i.e., 'lithium-rich' and 'oxygen-rich'

spinel, in which a homogeneous insertion/extraction reaction proceeds over the entire intercalated region.

3.5. A.c. impedance spectrum

As pointed out above, one factor that may cause capacity loss at high-operating temperatures is the electrolyte solution decomposition. To ascertain this model, the a.c. impedance technique was applied to investigate the interface reaction between the electrolyte solution and the electrode. Typical impedance spectra for the cell at open-circuit voltage (OCV) at both operating temperatures (25 and 50 °C) are shown in Figs. 7 and 9. Two semicircles are observed for the cell at 25 °C (curve (a), Fig. 7(a), enlarged in Fig. 7(b). Two different physical processes may be invoked to account for addition of another semicircle at the medium frequency for a porosity electrode in organic electrolyte solution: (i) adsorption of electrolyte (Li^+, PF_6^-) or electrolyte solvent on the surface of the electrode without charge transfer; (ii) formation of an ionically conducting, but electronically insulating, surface layer at the electrode surface, which is usually caused by the decomposition of solution when the cell is charged to a high voltage. In order to distinguish between these two possibilities, the cell charged to various oxidation depths were investigated by a.c. impedance spectra. The a.c. impedance spectra of the spinel electrode when the cell was charged to various oxidation depths are shown in Fig. 7. The semicircle at medium frequencies becomes smaller when more lithium ions are extracted from the structure of the spinel matrix. This would indicate partial dissolution of the adsorbed layers [9], not being caused by the formation of surface layer, since the diameter of the semicircle caused by the electrolyte decomposition should become larger when the cell is charged to a higher voltage. Finally, adsorption is greatly reduced so that the related semicircle disappears (curve (e), Fig. 7). The a.c. impedance spectra for the cell charged to $Li_{0.7}Mn_2O_4$ at various temperatures are given in Fig. 8. The semicircle at medium frequency becomes less visible as the operating temperature is raised. This is explained by the fact that high temperature is not so effective on the adsorption reaction as at low temperature. When the operating temperature of the

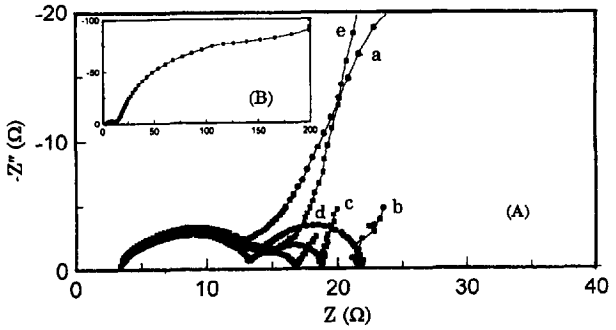

Fig. 7. A.c. impedance spectra for $LiMn_2O_4$ at various oxidation depths at 25 °C. Insert (B) and (a) OCV; (b) $Li_{0.9}Mn_2O_4$; (c) $Li_{0.6}Mn_2O_4$; (d) $Li_{0.4}Mn_2O_4$, and (e) $Li_{0.2}Mn_2O_4$.

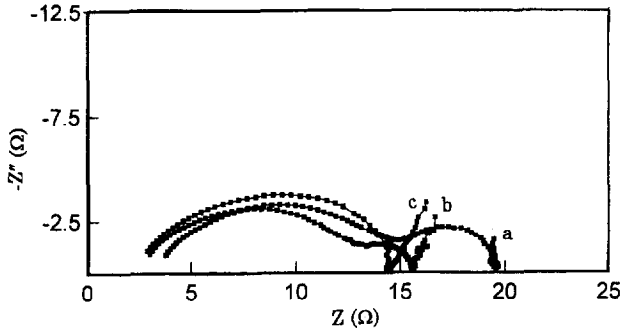

Fig. 8. A.c. impedance spectra for $LiMn_2O_4$ charged to $Li_{0.7}Mn_2O_4$ at various temperatures: (a) 25 °C; (b) 35 °C, and (c) 50 °C.

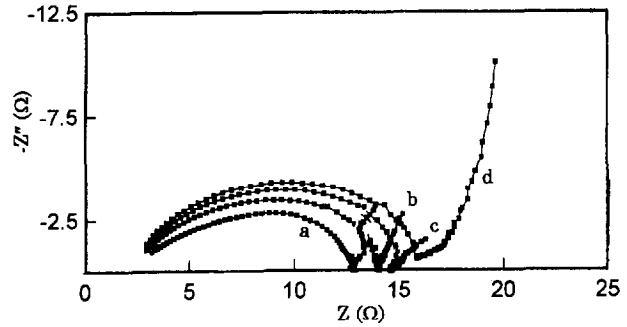

Fig. 9. A.c. impedance spectra for $LiMn_2O_4$ at various oxidation depths at 50 °C: (a) OCV; (b) $Li_{0.9}Mn_2O_4$; (c) $Li_{0.5}Mn_2O_4$, and (d) $Li_{0.3}Mn_2O_4$.

cell is raised to 50 °C, only one semicircle is detected at the OCV state (curve (a), Fig. 9). Further, when cells are charged to various oxidation depths, the dispersed-semicircle becomes larger. This may be associated with the formation of a surface layer caused by the decomposition of the electrolyte solution [10], where the possibility of an increment in the semicircle associated with the charge-transfer reaction (parallel of charge-transfer resistance, R_{ct} with double-layer capacitance, C_{dl}) is excluded, since the extraction reaction of Li^+ ions is almost constant, in which the semicircles at high frequency do not change when Li^+ ions are extracted at room temperature (Fig. 7). An increase in electrode resistance will cause a high cell polarization, and lead to an incomplete charging and, therefore, apparent capacity loss. A more detailed equivalent circuit analysis will be reported later [11]. The electrolyte decomposition depends on several factors in addition to the stability of the electrolyte, itself, e.g., the surface area of the electrode material, the surface area and the content of the conductor, and the limitation of the charge voltage, etc. Therefore, it is necessary to synthesize electrode material with a small surface area if the cell is used at high operating temperature.

4. Conclusions

In summary, the capacity fades faster on cycling at high operating temperature than that at low operating temperature. This is due mainly to an unstable two-phase structure co-

existing in the high-voltage region for lithium-ion insertion/extraction, and is also caused by the dissolution of manganese into the electrolyte solution and the decomposition of electrolyte solution.

The two-phase structure in the high-voltage region is very sensitive to working temperature. The low temperature can maintain the two-phase structure for lithium-ion insertion/extraction, while high temperature effectively forces it to transform to a one-phase structure in the high-voltage region.

Acknowledgements

The authors would like to thank the grants-in-aid for Scientific Research from the Japanese Ministry of Education (No. 06 555 188) for partial support of this research.

References

[1] J.M. Tarascon, W.R. McKinnon, F. Coowar, T.N. Bowmer, G. Amatucci and D. Guyomard, *J. Electrochem. Soc., 141* (1994) 1421.
[2] V. Manev, A. Momchilov, A. Nassalevska and A. Kozawa, *J. Power Sources, 41* (1993) 305.
[3] Y. Xia and M. Yoshio, *J. Power Sources, 56 (1995) 61; 57* (1995) 127.
[4] H. Hurimoto, K. Suzuoka, T. Murakami, Y. Xia, H. Nakamura and M. Yoshio, *J. Electrochem. Soc., 142* (1995) 2178.
[5] M.H. Rossouw, A. de Kock, L.A. de Picciotto and M.M. Thackeray, *Mater. Res. Bull., 25* (1990) 173.
[6] J. Barker, R. Pynenburg and R. Koksbang, *J. Power Sources, 52* (1994) 185.
[7] Y. Xia and M. Yoshio, *J. Electrochem. Soc., 127* (1996) 856.
[8] R.J. Gummow, A. de Kock and M.M. Thackery, *Solid State Ionics, 69* (1994) 59.
[9] L. Ba and B.E. Conway, *Electrochim. Acta, 38* (1993) 1803.
[10] D.H. Jang, J.Y. Shin and S.M. Oh, *J. Electrochem. Soc., 143* (1996) 2204.
[11] Y. Xia and M. Yoshio, unpublished data.